Prof. Yu Huang
State Key Lab of Loess and Quaternary Geology
Institute of Earth Environment, Chinese Academy
of Sciences, Xi'an, 710061, China
Tel./Fax: (86) 29-62336261
E-mail: huangyu@ieecas.cn

Sep. 30, 2022

Dear Prof. Kourtchev,

Revision for Manuscript ACP-2022-376

We thank you very much for giving us the opportunity to revise our manuscript. We highly appreciate the reviewers for their comments and suggestions on the manuscript entitled "**Oligomer formation from the gas-phase reactions of Criegee intermediates with hydroperoxide esters: mechanism and kinetics**". We have made revisions of our manuscript carefully according to the comments and suggestions of reviewers. The revised contents are marked in blue color. The response letter to reviewers is attached at the end of this cover letter.

We hope that the revised manuscript can meet the requirement of Atmospheric Chemistry & Physics. Any further modifications or revisions, please do not hesitate to contact us.

Look forward to hearing from you as soon as possible.

Best regards,

Yu Huang

Comments of reviewer #1

1. I have serious concerns with the calculation of rate constants for the barrierless 1,4 O-H insertion reactions. In the revised manuscript, the authors report using the Inverse Laplace Transform (ILT) method to compute rate constants for O-H insertion. However, what the ILT method in MESMER does is to convert thermal rate constants, as modeled by an Arrhenius expression, to microcanonical rate coefficients needed for master equation simulations. ILT cannot by itself predict rate constants; it is dependent on thermal rate constants that come from either experiment or theoretical methods like VTST, which was used in the original version of the manuscript.

Response: Based on the Reviewer's suggestion, the rate coefficients for the barrierless 1,4 O-H insertion reactions have been recalculated by employing the variable-reaction-coordinate variational transition-state theory (VRC-VTST) in the revised manuscript. The VRC-VTST calculations are performed with the potential surface obtained by direct dynamics using the M06-2X/6-311+G(2df,2p) method. Rate coefficients for the SCIs + HCOOH reactions are calculated using the E,J-resolved microcanonical variational theory (E,J-μVT) using a single-faceted dividing surface. In the VRC-VTST calculations, the reaction coordinate s is defined by pivot points, which are used to orientate the reactants 1 and 2. s is defined as the minimal value of r_{ij}, where r_{ij} is the distance between pivot points i and j, i is a pivot point on reactant 1 and j is a pivot point on reactant 2. Two of the pivot points are located at a distance $\pm d$ from the center of mass (COM) of SCIs, and the other two pivot points are located at a distance $\pm d$ from the COM of HCOOH with a fixed length of 0.05, 0.10, 0.15, 0.2 and 0.25 Å. Then, for a given choice of pivot points, the variationally lowest rate coefficients are minimized with respect to s at each of the temperatures. We observed that d=0.05 produces the best variation results and only its value is reported. The best variational results obtained for the barrierless 1,4 O-H insertion reactions are presented in Table S3-S6.

From Table S3, it can be seen that the total rate coefficients $k_{\text{tot-CH2OO}}$ of CH_2OO reaction with HCOOH are in excess of 1.0×10^{-10} cm^3 molecule^{-1} s^{-1}, and they exhibit a slightly negative temperature dependence in the temperature range of 273-400 K. At room temperature, $k_{\text{tot-CH2OO}}$ is estimated to be 1.29×10^{-10} cm^3 molecule^{-1} s^{-1}, which is in good agreement with the experimental values reported by Welz et al. (2014) ([$1.1 \pm 0.1 \times 10^{-10}$), Chung et al. (2019) ([1.4 ± 0.3] $\times 10^{-10}$),

and Peltola et al. (2020) ([1.0 ± 0.03] × 10^{-10}). k(TS$_{ent1}$) is approximately equal to $k_{tot-CH2OO}$ in the whole temperature range, and it decreases in the range of 1.34 × 10^{-10} (273 K) to 1.05 × 10^{-10} (400 K) cm^3 molecule^{-1} s^{-1} with increasing temperature. k(TS$_{ent1}$) is several orders of magnitude greater than k(TS$_{ent2}$), k(TS$_{ent3}$) and k(TS$_{ent4}$) over the temperature range from 273 to 400 K. The result again shows that the barrierless 1,4 O-H insertion reaction is predominant. Similar conclusion is also obtained from the results of the rate coefficients for the reactions of HCOOH with *anti*-CH$_3$CHOO, *syn*-CH$_3$CHOO and (CH$_3$)$_2$COO (Table S4-S6). At ambient temperature, the total rate coefficients of HCOOH reactions with *anti*-CH$_3$CHOO, *syn*-CH$_3$CHOO and (CH$_3$)$_2$COO are estimated to be 5.22, 2.18 and 3.97 × 10^{-10} cm^3 molecule^{-1} s^{-1}, respectively, which are consistent with the prior experimental measurements of 5 ± 3, 2.5 ± 0.3 and 4.5 ± 0.9 × 10^{-10} cm^3 molecule^{-1} s^{-1} (Welz et al., 2014; Sipilä et al., 2014).

Table S3 Rate coefficients (cm^3 molecule^{-1} s^{-1}) of each elementary pathway involved in the initiation reaction of CH$_2$OO with HCOOH computed at different temperatures

T/K	k (TS$_{ent1}$)	k (TS$_{ent2}$)	k (TS$_{ent3}$)	k (TS$_{ent4}$)	$k_{tot-CH2OO}$
273	1.34 × 10^{-10}	3.56 × 10^{-12}	1.03 × 10^{-22}	3.57 × 10^{-12}	1.41 × 10^{-10}
280	1.30 × 10^{-10}	2.94 × 10^{-12}	1.22 × 10^{-22}	3.12 × 10^{-12}	1.36 × 10^{-10}
298	1.25 × 10^{-10}	1.88 × 10^{-12}	2.18 × 10^{-22}	2.26 × 10^{-12}	1.29 × 10^{-10}
300	1.21 × 10^{-10}	1.80 × 10^{-12}	2.35 × 10^{-22}	2.20 × 10^{-12}	1.25 × 10^{-10}
320	1.17 × 10^{-10}	1.18 × 10^{-12}	4.86 × 10^{-22}	1.63 × 10^{-12}	1.20 × 10^{-10}
340	1.12 × 10^{-10}	8.16 × 10^{-13}	1.04 × 10^{-21}	1.26 × 10^{-12}	1.14 × 10^{-10}
360	1.11 × 10^{-10}	5.92 × 10^{-13}	2.20 × 10^{-21}	1.04 × 10^{-12}	1.13 × 10^{-10}
380	1.07 × 10^{-10}	4.48 × 10^{-13}	4.52 × 10^{-21}	8.23 × 10^{-13}	1.08 × 10^{-10}
400	1.05 × 10^{-10}	3.50 × 10^{-13}	9.01 × 10^{-21}	6.91 × 10^{-13}	1.06 × 10^{-10}

Table S4 Rate coefficients (cm^3 molecule^{-1} s^{-1}) of each elementary pathway involved in the initiation reaction of *anti*-CH$_3$CHOO with HCOOH computed at different temperatures

T/K	k (TS$_{ent1}$-*anti*)	k (TS$_{ent2}$-*anti*)	k (TS$_{ent3}$-*anti*)	k (TS$_{ent4}$-*anti*)	$k_{tot-anti}$
273	4.94 × 10^{-10}	4.23 × 10^{-11}	5.53 × 10^{-22}	6.12 × 10^{-11}	5.98 × 10^{-10}
280	4.82 × 10^{-10}	3.75 × 10^{-11}	6.73 × 10^{-22}	4.92 × 10^{-11}	5.69 × 10^{-10}
298	4.69 × 10^{-10}	2.34 × 10^{-11}	1.20 × 10^{-21}	2.95 × 10^{-11}	5.22 × 10^{-10}
300	4.56 × 10^{-10}	2.01 × 10^{-11}	1.29 × 10^{-21}	2.80 × 10^{-11}	5.04 × 10^{-10}

320	4.42×10^{-10}	1.48×10^{-11}	2.61×10^{-21}	1.72×10^{-11}	4.74×10^{-10}
340	4.28×10^{-10}	9.42×10^{-12}	5.36×10^{-21}	1.12×10^{-11}	4.49×10^{-10}
360	4.27×10^{-10}	7.04×10^{-12}	1.08×10^{-20}	7.77×10^{-12}	4.42×10^{-10}
380	4.14×10^{-10}	3.64×10^{-12}	2.12×10^{-20}	5.60×10^{-12}	4.23×10^{-10}
400	4.09×10^{-10}	2.02×10^{-12}	4.01×10^{-20}	4.18×10^{-12}	4.15×10^{-10}

Table S5 Rate coefficients (cm^3 molecule^{-1} s^{-1}) of each elementary pathway involved in the initiation reaction of *syn*-CH_3CHOO with HCOOH computed at different temperatures

T/K	k (TS$_{ent1}$-*syn*)	k (TS$_{ent2}$-*syn*)	k (TS$_{ent3}$-*syn*)	k (TS$_{ent4}$-*syn*)	$k_{tot\text{-}syn}$
273	2.34×10^{-10}	9.50×10^{-13}	4.58×10^{-27}	7.46×10^{-16}	2.35×10^{-10}
280	2.25×10^{-10}	8.03×10^{-13}	7.06×10^{-27}	6.43×10^{-16}	2.26×10^{-10}
298	2.17×10^{-10}	5.37×10^{-13}	8.92×10^{-26}	5.46×10^{-16}	2.18×10^{-10}
300	2.08×10^{-10}	5.15×10^{-13}	9.94×10^{-26}	4.58×10^{-16}	2.09×10^{-10}
320	1.99×10^{-10}	3.55×10^{-13}	3.03×10^{-25}	3.78×10^{-16}	1.99×10^{-10}
340	1.89×10^{-10}	2.57×10^{-13}	9.14×10^{-25}	3.05×10^{-16}	1.89×10^{-10}
360	1.88×10^{-10}	1.95×10^{-13}	2.64×10^{-24}	3.03×10^{-16}	1.88×10^{-10}
380	1.79×10^{-10}	1.53×10^{-13}	7.15×10^{-24}	2.43×10^{-16}	1.79×10^{-10}
400	1.76×10^{-10}	1.24×10^{-13}	1.82×10^{-23}	2.22×10^{-16}	1.76×10^{-10}

Table S6 Rate coefficients (cm^3 molecule^{-1} s^{-1}) of each elementary pathway involved in the initiation reaction of $(CH_3)_2OO$ with HCOOH computed at different temperatures

T/K	k (TS$_{ent1}$-*dim*)	k (TS$_{ent2}$-*dim*)	k (TS$_{ent3}$-*dim*)	k (TS$_{ent4}$-*dim*)	$k_{tot\text{-}dim}$
273	4.10×10^{-10}	6.81×10^{-12}	1.38×10^{-26}	4.37×10^{-15}	4.17×10^{-10}
280	4.02×10^{-10}	5.20×10^{-12}	2.24×10^{-26}	4.20×10^{-15}	4.07×10^{-10}
298	3.94×10^{-10}	2.78×10^{-12}	7.95×10^{-26}	4.03×10^{-15}	3.97×10^{-10}
300	3.86×10^{-10}	2.61×10^{-12}	9.18×10^{-26}	3.86×10^{-15}	3.89×10^{-10}
320	3.77×10^{-10}	1.44×10^{-12}	3.63×10^{-25}	3.71×10^{-15}	3.78×10^{-10}
340	3.68×10^{-10}	8.60×10^{-13}	1.33×10^{-24}	3.55×10^{-15}	3.69×10^{-10}
360	3.63×10^{-10}	5.48×10^{-13}	4.47×10^{-24}	3.54×10^{-15}	3.64×10^{-10}
380	3.59×10^{-10}	3.69×10^{-13}	1.37×10^{-23}	3.41×10^{-15}	3.59×10^{-10}

400	3.56×10^{-10}	2.60×10^{-13}	3.86×10^{-23}	3.37×10^{-15}	3.56×10^{-10}

Corresponding descriptions have been added in the page 7 line 180-195 and page 12 line 315-329 and page 12 line 333-355 of the revised manuscript:

The rate coefficients for the barrierless 1,4 O-H insertion reactions are computed by employing the variable-reaction-coordinate variational transition-state theory (VRC-VTST) (Bao and Truhlar, 2017), in which the potential energies are calculated by direct dynamics using the M06-2X/6-311+G(2df,2p) method. Rate coefficients for the SCIs + HCOOH reactions are calculated using the E,J-resolved microcanonical variational theory (E,J-μVT) using a single-faceted dividing surface. In the VRC-VTST calculations, the reaction coordinate s is defined by pivot points, which are used to orientate the reactants 1 and 2. s is defined as the minimal value of r_{ij}, where r_{ij} is the distance between pivot points i and j, i is a pivot point on reactant 1 and j is a pivot point on reactant 2. Two of the pivot points are located at a distance ±d from the center of mass (COM) of SCIs, and the other two pivot points are located at a distance ±d from the COM of HCOOH with a fixed length of 0.05, 0.10, 0.15, 0.2 and 0.25 Å. Then, for a given choice of pivot points, the variationally lowest rate coefficients are minimized with respect to s at each of the temperatures. We observed that d=0.05 produces the best variation results and only its value is reported in the present study.

The rate coefficients of each elementary pathway included in the initiation reactions of distinct SCIs with HCOOH are tabulated in Table S3-S6. The total rate coefficient is equal to the sum of the rate coefficient of each elementary pathway. As shown in Table S3, the total rate coefficients $k_{tot\text{-}CH2OO}$ of CH_2OO reaction with HCOOH are in excess of 1.0×10^{-10} cm^3 molecule^{-1} s^{-1}, and they exhibit a slightly negative temperature dependence in the temperature range of 273-400 K. At room temperature, $k_{tot\text{-}CH2OO}$ is estimated to be 1.29×10^{-10} cm^3 molecule^{-1} s^{-1}, which is in good agreement with the experimental values reported by Welz et al. (2014) ([1.1 ± 0.1] × 10^{-10}), Chung et al. (2019) ([1.4 ± 0.3] × 10^{-10}), and Peltola et al. (2020) ([1.0 ± 0.03] × 10^{-10}). $k(TS_{ent1})$ is approximately equal to $k_{tot\text{-}CH2OO}$ in the whole temperature range, and it decreases in the range of 1.34×10^{-10} (273 K) to 1.05×10^{-10} (400 K) cm^3 molecule^{-1} s^{-1} with increasing temperature. $k(TS_{ent1})$ is several orders of magnitude greater than $k(TS_{ent2})$, $k(TS_{ent3})$ and $k(TS_{ent4})$ over the temperature range from 273 to 400 K. The result again shows that the barrierless 1,4

O-H insertion reaction is predominant.

Equivalent to the case of the reaction of CH₂OO with HCOOH, the total rate coefficient k_{tot-anti} of anti-CH₃CHOO reaction with HCOOH also decreases slightly with the temperature increasing (Table S4). This table shows that Entry 1 is kinetically favored over Entry 2, 3 and 4, and Entry 2 is competitive with Entry 4 in the temperature range of 273-400 K. Similar conclusion is also obtained from the results of the rate coefficients for the reactions of syn-CH₃CHOO and (CH₃)₂COO with HCOOH that Entry 1 is the dominant pathway (Table S5-S6). It deserves mentioning that the competition of Entry 2 is significantly greater than that of Entry 4 in the syn-CH₃CHOO + HCOOH and (CH₃)₂COO + HCOOH systems. Based on the above discussions, it can be concluded that the relative importance of different pathways is highly dependent on the number and location of methyl substituents in the carbonyl oxides. Notably, the rate coefficient of each elementary pathway included in the anti-CH₃CHOO + HCOOH reaction is several orders of magnitude greater than that of the corresponding channel involved in the other SCIs + HCOOH systems. It is because that anti-CH₃CHOO is substantially more reactive toward HCOOH than other SCIs. Similar phenomenon has also observed from the reactivity of anti-CH₃CHOO toward water and SO₂ (Taatjes et al., 2013; Long et al., 2016; Huang et al., 2015; Cabezas and Endo, 2018). At ambient temperature, the total rate coefficients of HCOOH reactions with anti-CH₃CHOO, syn-CH₃CHOO and (CH₃)₂COO are estimated to be 5.22, 2.18 and 3.97 × 10⁻¹⁰ cm³ molecule⁻¹ s⁻¹, respectively, which are consistent with the prior experimental measurements of 5 ± 3, 2.5 ± 0.3 and 4.5 ± 0.9 × 10⁻¹⁰ cm³ molecule⁻¹ s⁻¹ (Welz et al., 2014; Sipilä et al., 2014).

2. The authors have done a good job providing a rationale for the trend in the exothermicities of the Criegee intermediate (CI) + HCOOH reactions. In the revised manuscript, the authors report computed enthalpies of formation for the four CIs under consideration, and relate the trend in these formation enthalpies to the trend in the CI + HCOOH reaction enthalpies.

Response: Thank the reviewer for his positive comments on the trend in the exothermicities of the reactions of distinct SCIs with HCOOH in the revised manuscript. The exothermicities of 1,4 O-H insertion reactions of distinct SCIs with HCOOH are assessed by the reaction enthalpies ($\Delta_r H^o_{298}$), which are defined as the difference between the enthalpies of formation ($\Delta_f H^o_{298}$) of the

products and reactants ($\Delta_r H^o_{298} = \sum\limits_{products} \Delta_f H^o_{298} - \sum\limits_{reactants} \Delta_f H^o_{298}$). The enthalpies of formation of

carbonyl oxides and hydroperoxide esters are estimated by using the isodesmic reaction method,

and the results are listed in Table S2. As seen in Table S2, the enthalpies of formation of carbonyl

oxides and hydroperoxide esters significantly decrease with increasing the number of methyl

groups. Notably, the decreased values in the enthalpies of formation of carbonyl oxides are greater

than those of hydroperoxide esters under the condition of the same number of methyl groups. For

example, the enthalpy of formation of *anti*-CH$_3$CHOO decreases by 12.95 kcal·mol^{-1} compared to

the enthalpy of formation of CH$_2$OO (23.23 kcal·mol^{-1}), and the enthalpy of formation of Pent1b

decreases by 12.12 kcal·mol^{-1} compared to the enthalpy of formation of Pent1a (-112.08

kcal·mol^{-1}). The reaction enthalpies of the reactions of distinct SCIs with HCOOH decrease in the

order of -44.69 (CH$_2$OO + HCOOH → Pent1a) < -43.86 (*anti*-CH$_3$CHOO + HCOOH → Pent1b)

< -38.13 (*syn*-CH$_3$CHOO + HCOOH → Pent1c) < -37.12 kcal·mol^{-1} ((CH$_3$)$_2$COO + HCOOH →

Pent1d), indicating that the reaction enthalpies are highly dependent on the number and location of

methyl groups. The trend in reaction enthalpies is consistent with the trend in the enthalpies of

formation of carbonyl oxides.

Table S2 Enthalpies of formation ($\Delta_f H^o_{298}$) for the various carbonyl oxides and hydroperoxide

esters computed at the CCSD(T)//M06-2X/6-311+G(2df,2p) level of theory

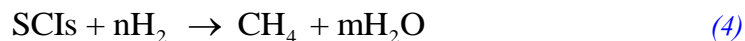| Species	Cal (kcal·mol^{-1})	Refs. (kcal·mol^{-1})
CH$_2$OO	23.23	22.92[a] 24.59[b]
anti-CH$_3$OO	10.28	
syn-CH$_3$CHOO	6.73	
(CH$_3$)$_2$COO	-6.77	
HCOOH		-90.62 (exp)
HC(O)OCH$_2$OOH (Pent1a)	-112.08	
HC(O)OCH(CH$_3$)OOH (Pent1b)	-124.20	
HC(O)OCH(CH$_3$)OOH (Pent1c)	-122.02	
HC(O)OC(CH$_3$)$_2$OOH (Pent1d)	-134.51	

Exp is taken from NIST Chemistry Webbook

[a] the value is obtained at the G4 level of theory (Chen et al., 2016)

[b] the value is obtained at the W3-F12 level of theory (Karton et al., 2013)

Corresponding descriptions have been added in the page 10 line 253-283 of the revised manuscript:

The exothermicities of 1,4 O-H insertion reactions of distinct SCIs with HCOOH are assessed by the reaction enthalpies ($\Delta_r H_{298}^o$), which are defined as the difference between the enthalpies of formation ($\Delta_f H_{298}^o$) of the products and reactants ($\Delta_r H_{298}^o = \sum\limits_{products} \Delta_f H_{298}^o - \sum\limits_{reactants} \Delta_f H_{298}^o$). To the best of our knowledge, there are no literature values available on the enthalpies of formation of carbonyl oxides and hydroperoxide esters except the simplest carbonyl oxide CH_2OO. Therefore, the isodesmic reaction method is adopted to obtain the enthalpies of formation, and the results are listed in Table S2. An isodesmic reaction is a hypothetical reaction, in which the type of chemical bonds in the reactants is the similar as that of chemical bonds in the products. The following isodesmic reaction is constructed because the experimental values of H_2, CH_4 and H_2O are available ($\Delta_f H_{298}^o$ (H_2) = 0.00 kcal·mol⁻¹; $\Delta_f H_{298}^o$ (CH_4) = -17.82 kcal·mol⁻¹; $\Delta_f H_{298}^o$ (H_2O) = -57.79 kcal·mol⁻¹).

$$SCIs + nH_2 \; \rightarrow \; CH_4 + mH_2O \qquad (4)$$

As seen in Table S2, the enthalpy of formation of CH_2OO is calculated to be 23.23 kcal·mol⁻¹, which is in good agreement with the available literature values (Chen et al., 2016; Karton et al., 2013). This result implies that the theoretical method employed herein is reasonable to predict the thermochemical parameters. The enthalpies of formation of carbonyl oxides and hydroperoxide esters significantly decrease with increasing the number of methyl groups. Notably, the decreased values in the enthalpies of formation of carbonyl oxides are greater than those of hydroperoxide esters under the condition of the same number of methyl groups. For example, the enthalpy of formation of anti-CH_3CHOO decreases by 12.95 kcal·mol⁻¹ compared to the enthalpy of formation of CH_2OO (23.23 kcal·mol⁻¹), and the enthalpy of formation of Pent1b decreases by 12.12 kcal·mol⁻¹ compared to the enthalpy of formation of Pent1a (-112.08 kcal·mol⁻¹). The reaction enthalpies of the reactions of distinct SCIs with HCOOH decrease in the order of -44.69 (CH_2OO + HCOOH $\rightarrow$ Pent1a) < -43.86 (anti-CH_3CHOO + HCOOH $\rightarrow$ Pent1b) < -38.13 (syn-CH_3CHOO + HCOOH $\rightarrow$ Pent1c) < -37.12 kcal·mol⁻¹ ((CH_3)$_2$COO + HCOOH $\rightarrow$ Pent1d), indicating that the reaction enthalpies are highly dependent on the number and location of methyl

groups. The trend in reaction enthalpies is consistent with the trend in the enthalpies of formation of carbonyl oxides.

3. In the original version of the manuscript, the authors had already answered the question I posed: how fast do all four CIs under consideration react with the most important bimolecular reaction partners in the atmosphere. I apologize for missing Table 2.

Response: As the Reviewer's said, the reactions with trace species (e.g., H_2O, HCOOH and SO_2) are expected to be the dominant chemical sinks for the considered all four SCIs (CH_2OO, *syn*-CH_3CHOO, *anti*-CH_3CHOO and $(CH_3)_2COO$) in the atmosphere. The reported concentrations of coreactant, the rate coefficients k, and the effective pseudo-first-order rate constants (k_{eff} = k[coreactant]) for the reactions of distinct SCIs with H_2O, HCOOH, SO_2 are summarized in Table 2. As seen in Table 2, the rate coefficient of a particular SCI reaction with trace species is strongly dependent on its structure. The methyl group substitution may alter the rate coefficient by several to tens of times. The atmospheric concentrations of H_2O, HCOOH and SO_2 in the tropical forest environments are measured to be $3.9\text{-}6.1 \times 10^{17}$, $5.0\text{-}10 \times 10^{10}$, and $1.7\text{-}9.0 \times 10^{10}$ molecules cm^{-3}, respectively (Vereecken et al., 2012). For the reactions of CH_2OO with H_2O, HCOOH, and SO_2, the experimental rate coefficients are determined to be $< 1.5 \times 10^{-15}$, $[1.1 \pm 0.1] \times 10^{-10}$, and $[3.9 \pm 0.7] \times 10^{-11}$ cm^3 molecule^{-1} s^{-1}, respectively (Welz et al., 2012 and 2014; Chao et al., 2015), which translate into $k_{eff(CH2OO+H2O)}$, $k_{eff(CH2OO+HCOOH)}$ and $k_{eff(CH2OO+SO2)}$ of $5.9\text{-}9.2 \times 10^2$, $5.5\text{-}11$, and $0.7\text{-}3.5$ s^{-1}, respectively. The result reveals that the reaction of CH_2OO with H_2O is the most important bimolecular reaction. $k_{eff(CH2OO+HCOOH)}$ is greater by a factor of 3-8 than $k_{eff(CH2OO+SO2)}$, indicating that CH_2OO reaction with HCOOH is favored over reaction with SO_2. Similar conclusion is also obtained from the results of k_{eff} for the reactions of *anti*-CH_3CHOO, *syn*-CH_3CHOO and $(CH_3)_2COO$ with H_2O, HCOOH and SO_2 that SCIs reactions with H_2O are faster than with HCOOH, which, in turn, are faster than with SO_2.

Table 2 The reported concentrations of coreactant, the rate coefficients k, and the effective pseudo-first-order rate constants (k_{eff} = k[coreactant]) for distinct SCI reactions with HPMF, H_2O, HCOOH and SO_2 at the tropical forest environments

SCIs	Coreactant	[Coreactant] (molecules cm^{-3})	k (cm^3 molecule^{-1} s^{-1})	k_{eff} (s^{-1})	Reference
CH_2OO	H_2O	$3.9\text{-}6.1 \times 10^{17}$	$< 1.5 \times 10^{-15}$	$5.9\text{-}9.2 \times 10^2$	Chao et al., (2015)

	HCOOH	$5.0\text{-}10.0 \times 10^{10}$	$[1.1 \pm 0.1] \times 10^{-10}$	5.5-11	Welz et al., (2014)
	SO_2	$1.7\text{-}9.0 \times 10^{10}$	$[3.9 \pm 0.7] \times 10^{-11}$	0.7-3.5	Welz et al., (2012)
	HPMF	-	2.7×10^{-11}	-	This work
	H_2O	$3.9\text{-}6.1 \times 10^{17}$	$[1.0 \pm 0.4] \times 10^{-14}$	$3.9\text{-}6.1 \times 10^{3}$	Taatjes et al., (2013)
anti-CH_3CHOO	HCOOH	$5.0\text{-}10.0 \times 10^{10}$	$[5 \pm 3] \times 10^{-10}$	25.0-50.0	Welz et al., (2014)
	SO_2	$1.7\text{-}9.0 \times 10^{10}$	$[6.7 \pm 1.0] \times 10^{-11}$	1.1-6.0	Taatjes et al., (2013)
	HPMF	-	3.3×10^{-10}	-	This work
	H_2O	$3.9\text{-}6.1 \times 10^{17}$	$< 4.0 \times 10^{-15}$	$1.6\text{-}2.4 \times 10^{3}$	Taatjes et al., (2013)
syn-CH_3CHOO	HCOOH	$5.0\text{-}10.0 \times 10^{10}$	$[2.5 \pm 0.3] \times 10^{-10}$	12.5-25.0	Welz et al., (2014)
	SO_2	$1.7\text{-}9.0 \times 10^{10}$	$[2.4 \pm 0.3] \times 10^{-11}$	0.4-2.2	Taatjes et al., (2013)
	HPMF	-	1.7×10^{-13}	-	This work
	H_2O	$3.9\text{-}6.1 \times 10^{17}$	$< 1.5 \times 10^{-16}$	58.5-91.5	Huang et al., (2015)
$(CH_3)_2COO$	HCOOH	$5.0\text{-}10.0 \times 10^{10}$	4.5×10^{-10}	22.5-45.0	Sipilä et al., (2014)
	SO_2	$1.7\text{-}9.0 \times 10^{10}$	1.3×10^{-10}	2.2-11.7	Huang et al., (2015)
	HPMF	-	2.2×10^{-11}	-	This work
	H_2O	$3.9\text{-}6.1 \times 10^{17}$	$< 4.0 \times 10^{-17}$	15.6-24.4	Caravan et al., (2020)
syn-trans-MVK -OO	HCOOH	$5.0\text{-}10.0 \times 10^{10}$	$[3.0 \pm 0.1] \times 10^{-10}$	15.0-30.0	Caravan et al., (2020)
	SO_2	$1.7\text{-}9.0 \times 10^{10}$	$[4.2 \pm 0.6] \times 10^{-11}$	0.7-3.8	Caravan et al., (2020)
	HPMF	-	3.0×10^{-11}	-	This work

Corresponding descriptions have been revised in the page 23 line 581-603 of the revised manuscript:

It is of interest to assess whether the reactions of distinct SCIs with HPMF can compete well

with the losses to reactions with trace species (e.g., H_2O, HCOOH and SO_2), because it is well known that the reactions with trace species are expected to be the dominant chemical sinks for SCIs in the atmosphere (Taatjes et al., 2013; Long et al., 2016). The reported concentrations of coreactant, the rate coefficients k, and the effective pseudo-first-order rate constants (k_{eff} = k[coreactant]) for the reactions of distinct SCIs with H_2O, HCOOH, SO_2, and HPMF are summarized in Table 2. As seen in Table 2, the rate coefficient of a particular SCI reaction with trace species is strongly dependent on its structure. The methyl group substitution may alter the rate coefficient by several to tens of times. The atmospheric concentrations of H_2O, HCOOH and SO_2 in the tropical forest environments are measured to be 3.9-6.1 $\times$ 10^{17}, 5.0-10 $\times$ 10^{10}, and 1.7-9.0 $\times$ 10^{10} molecules cm^{-3}, respectively (Vereecken et al., 2012). For the reactions of CH_2OO with H_2O, HCOOH, and SO_2, the experimental rate coefficients are determined to be < 1.5 $\times$ 10^{-15}, [1.1 ± 0.1] $\times$ 10^{-10}, and [3.9 ± 0.7] $\times$ 10^{-11} cm^3 $molecule^{-1}$ s^{-1}, respectively (Welz et al., 2012 and 2014; Chao et al., 2015), which translate into $k_{eff(CH2OO+H2O)}$, $k_{eff(CH2OO+HCOOH)}$ and $k_{eff(CH2OO+SO2)}$ of 5.9-9.2 $\times$ 10^2, 5.5-11, and 0.7-3.5 s^{-1}, respectively. The result reveals that the reaction of CH_2OO with H_2O is the most important bimolecular reaction. $k_{eff(CH2OO+HCOOH)}$ is greater by a factor of 3-8 than $k_{eff(CH2OO+SO2)}$, indicating that CH_2OO reaction with HCOOH is favored over reaction with SO_2. Similar conclusion is also obtained from the results of k_{eff} for the reactions of anti-CH_3CHOO, syn-CH_3CHOO and $(CH_3)_2COO$ with H_2O, HCOOH and SO_2 that SCIs reactions with H_2O are faster than with HCOOH, which, in turn, are faster than with SO_2.

4. The authors now quantify the pseudo-first-order rate constants for the reaction of CIs with HPMF with the more accurate assumption that the concentration of HPMF will be equal to the atmospheric concentration of CIs.

Response: As the Reviewer's said, we make the more accurate assumption that the concentration of HPMF is approximately equal to the atmospheric concentration of SCIs in the calculation of the pseudo-first-order rate constants for the bimolecular reaction of SCIs with HPMF. It is mainly because that the SCIs is the deficient reactant in the bimolecular reaction of SCIs with HCOOH. The competition between SCIs + HPMF and SCIs + trace species (e.g., H_2O, HCOOH and SO_2) reactions is taken into consideration in the revised manuscript, because it is well known that the reactions with trace species are expected to be the dominant chemical sinks

for SCIs in the atmosphere (Taatjes et al., 2013; Long et al., 2016). The reported concentrations of coreactant, the rate coefficients k, and the effective pseudo-first-order rate constants (k_{eff} = k[coreactant]) for the reactions of distinct SCIs with H_2O, HCOOH, SO_2, and HPMF are summarized in Table 2. As seen in Table 2, the rate coefficient of a particular SCI reaction with trace species is strongly dependent on its structure. The methyl group substitution may alter the rate coefficient by several to tens of times. The atmospheric concentrations of H_2O, HCOOH and SO_2 in the tropical forest environments are measured to be 3.9-6.1 × 10^{17}, 5.0-10 × 10^{10}, and 1.7-9.0 × 10^{10} molecules cm^{-3}, respectively (Vereecken et al., 2012). For the reactions of CH_2OO with H_2O, HCOOH, and SO_2, the experimental rate coefficients are determined to be < 1.5 × 10^{-15}, [1.1 ± 0.1] × 10^{-10}, and [3.9 ± 0.7] × 10^{-11} cm^3 molecule^{-1} s^{-1}, respectively (Welz et al., 2012 and 2014; Chao et al., 2015), which translate into $k_{eff(CH2OO+H2O)}$, $k_{eff(CH2OO+HCOOH)}$ and $k_{eff(CH2OO+SO2)}$ of 5.9-9.2 × 10^2, 5.5-11, and 0.7-3.5 s^{-1}, respectively. The result reveals that the reaction of CH_2OO with H_2O is the most important bimolecular reaction. $k_{eff(CH2OO+HCOOH)}$ is greater by a factor of 3-8 than $k_{eff(CH2OO+SO2)}$, indicating that CH_2OO reaction with HCOOH is favored over reaction with SO_2. Similar conclusion is also obtained from the results of k_{eff} for the reactions of *anti*-CH_3CHOO, *syn*-CH_3CHOO and $(CH_3)_2COO$ with H_2O, HCOOH and SO_2 that SCIs reactions with H_2O are faster than with HCOOH, which, in turn, are faster than with SO_2.

To the best of our knowledge, the atmospheric concentration of HPMF has not been reported up to now. We assume that the concentration of HPMF is approximately equal to the atmospheric concentration of SCIs, since the SCIs is the deficient reactant in the bimolecular reaction of SCIs with HCOOH. Previous model-measurement studies have estimated the surface-level SCIs concentrations in the range of 1.0 × 10^4 to 1.0 × 10^5 molecules cm^{-3} (Khan et al., 2018; Novelli et al., 2017). The room temperature rate coefficient for the reaction of CH_2OO with HPMF is calculated to be 2.7 × 10^{-11} cm^3 molecule^{-1} s^{-1}, which translates into $k_{eff(CH2OO+HPMF)}$ of 2.7-27 × 10^{-7} s^{-1}. $k_{eff(CH2OO+HPMF)}$ is several orders of magnitude lower than $k_{eff(CH2OO+H2O)}$, $k_{eff(CH2OO+HCOOH)}$ and $k_{eff(CH2OO+SO2)}$. Similar conclusion is also obtained from the reactions of *anti*-CH_3CHOO, *syn*-CH_3CHOO and $(CH_3)_2COO$ with HPMF.

Corresponding descriptions have been added in the page 23 line 581-600 and page 24 line 601-615 of the revised manuscript:

It is of interest to assess whether the reactions of distinct SCIs with HPMF can compete well

with the losses to reactions with trace species (e.g., H_2O, HCOOH and SO_2), because it is well known that the reactions with trace species are expected to be the dominant chemical sinks for SCIs in the atmosphere (Taatjes et al., 2013; Long et al., 2016). The reported concentrations of coreactant, the rate coefficients k, and the effective pseudo-first-order rate constants (k_{eff} = k[coreactant]) for the reactions of distinct SCIs with H_2O, HCOOH, SO_2, and HPMF are summarized in Table 2. As seen in Table 2, the rate coefficient of a particular SCI reaction with trace species is strongly dependent on its structure. The methyl group substitution may alter the rate coefficient by several to tens of times. The atmospheric concentrations of H_2O, HCOOH and SO_2 in the tropical forest environments are measured to be 3.9-6.1 × 10^{17}, 5.0-10 × 10^{10}, and 1.7-9.0 × 10^{10} molecules cm^{-3}, respectively (Vereecken et al., 2012). For the reactions of CH_2OO with H_2O, HCOOH, and SO_2, the experimental rate coefficients are determined to be < 1.5 × 10^{-15}, [1.1 ± 0.1] × 10^{-10}, and [3.9 ± 0.7] × 10^{-11} cm^3 molecule^{-1} s^{-1}, respectively (Welz et al., 2012 and 2014; Chao et al., 2015), which translate into $k_{eff(CH2OO+H2O)}$, $k_{eff(CH2OO+HCOOH)}$ and $k_{eff(CH2OO+SO2)}$ of 5.9-9.2 × 10^2, 5.5-11, and 0.7-3.5 s^{-1}, respectively. The result reveals that the reaction of CH_2OO with H_2O is the most important bimolecular reaction. $k_{eff(CH2OO+HCOOH)}$ is greater by a factor of 3-8 than $k_{eff(CH2OO+SO2)}$, indicating that CH_2OO reaction with HCOOH is favored over reaction with SO_2. Similar conclusion is also obtained from the results of k_{eff} for the reactions of anti-CH_3CHOO, syn-CH_3CHOO and $(CH_3)_2COO$ with H_2O, HCOOH and SO_2 that SCIs reactions with H_2O are faster than with HCOOH, which, in turn, are faster than with SO_2.

According to the results shown in the Table 2, the room temperature rate coefficient for the reaction of CH_2OO with HPMF is calculated to be 2.7 × 10^{-11} cm^3 molecule^{-1} s^{-1}. However, to the best of our knowledge, the atmospheric concentration of HPMF has not been reported up to now. We assume that the concentration of HPMF is approximately equal to the atmospheric concentration of SCIs, since the SCIs is the deficient reactant in the bimolecular reaction of SCIs with HCOOH. Previous model-measurement studies have estimated the surface-level SCIs concentrations in the range of 1.0 × 10^4 to 1.0 × 10^5 molecules cm^{-3} (Khan et al., 2018; Novelli et al., 2017). $k_{eff(CH2OO+HPMF)}$ is calculated to be 2.7-27 × 10^{-7} s^{-1}, which is several orders of magnitude lower than $k_{eff(CH2OO+H2O)}$, $k_{eff(CH2OO+HCOOH)}$ and $k_{eff(CH2OO+SO2)}$. Similar conclusion is also obtained from the reactions of anti-CH_3CHOO, syn-CH_3CHOO and $(CH_3)_2COO$ with HPMF.

5. I commend the authors for the work they have done to include estimates of vapor pressures and saturation concentrations in the revised manuscript. One question I have is why, for the nCH_2OO + HCOOH series, the vapor pressures do not decrease monotonically with increasing n.

Response: Based on the Reviewer's suggestion, the vapour pressure of the adduct products formed from the successive reactions of SCIs with HCOOH has been recalculated in the revised manuscript. To further evaluate the reliability of the considered methods for the calculations of vapor pressure, some selected compounds with experimental data are calculated by using the combination of boiling point and vapour pressure method proposed by Nannoolal et al. (2004 and 2008) (Nan-Nan) and the EVAPORATION method proposed by Compernolle et al. (2011) The calculated results are listed in Table R1. This table shows that the saturated vapour pressure (P^0) obtained using the EVAPORATION method is consistent with the experimentally reported ones. The P^0 obtained using the Nan-Nan method is about one order of magnitude greater than the experimental data, suggesting that the Nan-Nan method overestimates the saturated vapour pressure. Therefore, in the revised manuscript, the saturated vapour pressure of adduct products at room temperature is estimated by using the EVAPORATION method, and the results are summarized in Table S8. As show in Table S8, the P^0 of the adduct products decreases significantly as the number of SCIs is increased. Notably, the P^0 of the adduct products decreases when the size of SCIs increases. For example, the P^0 of the adduct product $HC(O)O(CH_2OO)_3H$ in the nCH_2OO + HCOOH reaction is estimated to be 3.41×10^{-5} atm, which is greater than those of the corresponding adduct products in the n$anti$-CH_3CHOO + HCOOH (4.73×10^{-6} atm), nsyn-CH_3CHOO + HCOOH (4.73×10^{-6} atm), and n$(CH_3)_2COO$ + HCOOH (1.03×10^{-6} atm) reactions by 7.21, 7.21 and 33.11 times, respectively.

A classify scheme of various organic compounds is based on their volatility, as presented by Donahue et al. (2012) The volatility of organic compounds is described by their effective saturation concentrations. The saturated concentrations (c^0) of the adduct products formed from the successive reactions of SCIs with HCOOH are listed in Table S8. As shown in Table S8, the c^0 of the adduct products decrease significantly as the number of SCIs is increased. It deserves mentioning that the c^0 of the adduct products decrease with increasing the size of SCIs. For the nCH_2OO + HCOOH reaction, the c^0 of the adduct products are estimated to be 1.03×10^8 (n=1), 5.42×10^6 (n=2), 2.53×10^5 (n=3), 1.11×10^4 (n=4) and 4.67×10^2 (n=5) ug/m^3, respectively.

According to the Volatility Basis Set (VBS) of organic compounds (Donahue et al., 2012), the adduct products belong to volatile organic compounds (VOC, $c^0 > 3 \times 10^6$ ug/m^3) when the number of SCIs is less than or equal to two, while they belong to intermediate volatility organic compounds (IVOC, $300 < c^0 < 3 \times 10^6$ ug/m^3) when the number of SCIs is greater than or equal to three. Similarly, the adduct products in the n$anti$-CH$_3$CHOO + HCOOH, nsyn-CH$_3$CHOO + HCOOH, and n(CH$_3$)$_2$COO + HCOOH reactions belong to IVOC when the number of SCIs ranges from 2 to 4, whereas they belong to semivolatile organic compounds (SVOC, $0.3 < c^0 < 300$ ug/m^3) when the number of SCIs is equal to 5. Based on the above discussions, it can be concluded that the volatility of the adduct products is significantly affected by the number and size of SCIs in the successive reaction of SCIs with HCOOH. The formed adduct products may participate in the formation and growth processes of organic new particle in the atmosphere.

Table R1 Saturated vapour pressure (P^0) of some selected compounds predicted by using the Nan-Nan and EVAPORATION methods

Compounds	Nan-Nan (Pa)	EVAPORATION (Pa)	experimental data (Pa)
methanol	5.81×10^5	1.58×10^4	1.67×10^4
ethanol	2.27×10^4	8.12×10^3	7.96×10^3
isoprene	3.51×10^5	7.35×10^4	7.33×10^4
cyclohexene	5.61×10^4	1.15×10^4	1.30×10^4
n-hexane	1.41×10^5	2.00×10^4	2.02×10^4
n-heptane	4.55×10^4	6.12×10^3	6.09×10^3
methylbenzene	2.17×10^4	3.16×10^3	3.79×10^3

Table S8 Predicted saturated vapour pressure (P^0) and saturated concentrations (c^0) for the adduct products of the successive reactions of SCIs with HCOOH

	formula	P^0 (atm)	c^0 (ug/m^3)
n CH$_2$OO + HCOOH			
n = 1	HC(O)OCH$_2$OOH	2.77×10^{-2}	1.03×10^8
n = 2	HC(O)O(CH$_2$OO)$_2$H	9.73×10^{-4}	5.42×10^6
n = 3	HC(O)O(CH$_2$OO)$_3$H	3.41×10^{-5}	2.53×10^5
n = 4	HC(O)O(CH$_2$OO)$_4$H	1.20×10^{-6}	1.11×10^4
n = 5	HC(O)O(CH$_2$OO)$_5$H	4.19×10^{-8}	4.67×10^2
n $anti$-CH$_3$CHOO + HCOOH			
n = 1	HC(O)OCH(CH$_3$)OOH	1.44×10^{-2}	6.15×10^7

n = 2	HC(O)O(CH(CH$_3$)OO)$_2$H	2.61×10^{-4}	1.75×10^{6}
n = 3	HC(O)O(CH(CH$_3$)OO)$_3$H	4.73×10^{-6}	4.32×10^{4}
n = 4	HC(O)O(CH(CH$_3$)OO)$_4$H	8.59×10^{-8}	9.92×10^{2}
n = 5	HC(O)O(CH(CH$_3$)OO)$_5$H	1.56×10^{-9}	2.18×10^{1}
n syn-CH$_3$CHOO + HCOOH			
n = 1	HC(O)OCH(CH$_3$)OOH	1.44×10^{-2}	6.15×10^{7}
n = 2	HC(O)O(CH(CH$_3$)OO)$_2$H	2.61×10^{-4}	1.75×10^{6}
n = 3	HC(O)O(CH(CH$_3$)OO)$_3$H	4.73×10^{-6}	4.32×10^{4}
n = 4	HC(O)O(CH(CH$_3$)OO)$_4$H	8.59×10^{-8}	9.92×10^{2}
n = 5	HC(O)O(CH(CH$_3$)OO)$_5$H	1.56×10^{-9}	2.18×10^{1}
n (CH$_3$)$_2$COO + HCOOH			
n = 1	HC(O)OC(CH$_3$)$_2$OOH	1.86×10^{-3}	9.02×10^{6}
n = 2	HC(O)O(C(CH$_3$)$_2$OO)$_2$H	4.38×10^{-5}	3.43×10^{5}
n = 3	HC(O)O(C(CH$_3$)$_2$OO)$_3$H	1.03×10^{-6}	1.11×10^{4}
n = 4	HC(O)O(C(CH$_3$)$_2$OO)$_4$H	2.42×10^{-8}	3.35×10^{2}
n = 5	HC(O)O(C(CH$_3$)$_2$OO)$_5$H	5.70×10^{-10}	9.57×10^{0}

Corresponding descriptions have been added in the page 26 line 649-681 of the revised manuscript:

The saturated vapour pressure (P^0) of the adduct products formed from the successive reactions of SCIs with HCOOH is estimated by using the EVAPORATION method proposed by Compernolle et al. (2011), and the room temperature results are summarized in Table S8. This table shows that the P^0 of the adduct products decreases significantly as the number of SCIs is increased. Notably, the P^0 of the adduct products decreases when the size of SCIs increases. For example, the P^0 of the adduct product HC(O)O(CH$_2$OO)$_3$H in the nCH$_2$OO + HCOOH reaction is estimated to be 3.41×10^{-5} atm, which is greater than those of the corresponding adduct products in the nanti-CH$_3$CHOO + HCOOH (4.73×10^{-6} atm), nsyn-CH$_3$CHOO + HCOOH (4.73×10^{-6} atm), and n(CH$_3$)$_2$COO + HCOOH (1.03×10^{-6} atm) reactions by 7.21, 7.21 and 33.11 times, respectively.

A classify scheme of various organic compounds is based on their volatility, as presented by Donahue et al. (2012) The volatility of organic compounds is described by their effective saturation concentrations. The saturated concentrations (c^0) of the adduct products formed from the successive reactions of SCIs with HCOOH are listed in Table S8. As shown in Table S8, the c^0 of the adduct products decrease significantly as the number of SCIs is increased. It deserves mentioning that the c^0 of the adduct products decrease with increasing the size of SCIs. For the

nCH₂OO + HCOOH reaction, the c^0 of the adduct products are estimated to be 1.03×10^8 (n=1),

5.42×10^6 (n=2), 2.53×10^5 (n=3), 1.11×10^4 (n=4) and 4.67×10^2 (n=5) ug/m³, respectively.

According to the Volatility Basis Set (VBS) of organic compounds (Donahue et al., 2012), the

adduct products belong to volatile organic compounds (VOC, $c^0 > 3 \times 10^6$ ug/m³) when the

number of SCIs is less than or equal to two, while they belong to intermediate volatility organic

compounds (IVOC, $300 < c^0 < 3 \times 10^6$ ug/m³) when the number of SCIs is greater than or equal to

three. Similarly, the adduct products in the nanti-CH₃CHOO + HCOOH, nsyn-CH₃CHOO +

HCOOH, and n(CH₃)₂COO + HCOOH reactions belong to IVOC when the number of SCIs

ranges from 2 to 4, whereas they belong to semivolatile organic compounds (SVOC, $0.3 < c^0 <$

300 ug/m³) when the number of SCIs is equal to 5. Based on the above discussions, it can be

concluded that the volatility of the adduct products is significantly affected by the number and size

of SCIs in the successive reaction of SCIs with HCOOH. The formed adduct products may

participate in the formation and growth processes of organic new particle in the atmosphere.

6. Finally, the Conclusion to the revised manuscript should contain some discussion of the atmospheric significance of the reactions they have considered. Key points to address are the very small pseudo-first-order rate constants for the CI + hydroperoxy ester reaction and the likelihood of oligomers of the dimethyl CI to be IVOCs.

Response: Based on the Reviewer's suggestion, the effective pseudo-first-order rate constants for the reactions of SCIs with hydroperoxide ester and the saturated vapour pressure and saturated concentration of the formed oligomers have been added in the Conclusion of the revised manuscript.

(e) In the tropical forest environments, the effective pseudo-first-order rate constants for the reactions of distinct SCIs with HPMF ($k_{\text{eff(SCIs+HPMF)}}$) are several orders of magnitude lower than those for the reactions of distinct SCIs with H₂O ($k_{\text{eff(SCIs+H2O)}}$), HCOOH ($k_{\text{eff(SCIs+HCOOH)}}$) and SO₂ ($k_{\text{eff(SCIs+SO2)}}$). $k_{\text{eff(SCIs+H2O)}}$ is greater than $k_{\text{eff(SCIs+HCOOH)}}$, which, in turn, is greater than $k_{\text{eff(SCIs+SO2)}}$.

(f) The saturated vapour pressure and saturated concentration of the adduct products formed from the successive reactions of SCIs with HCOOH decrease significantly as the number of SCIs is increased. The adduct products in the nCH₂OO + HCOOH reactions belong to IVOC when the number of SCIs is greater than or equal to 3. The adduct products in the n*anti*-CH₃CHOO +

HCOOH, nsyn-CH$_3$CHOO + HCOOH, and n(CH$_3$)$_2$COO + HCOOH reactions belong to IVOC when the number of SCIs ranges from 2 to 4, whereas they belong to SVOC when the number of SCIs is equal to 5.

Corresponding descriptions have been added in the page 15 line 414-421 of the revised manuscript:

(e) In the tropical forest environments, the effective pseudo-first-order rate constants for the reactions of distinct SCIs with HPMF ($k_{eff(SCIs+HPMF)}$) are several orders of magnitude lower than those for the reactions of distinct SCIs with H$_2$O ($k_{eff(SCIs+H2O)}$), HCOOH ($k_{eff(SCIs+HCOOH)}$) and SO$_2$ ($k_{eff(SCIs+SO2)}$). $k_{eff(SCIs+H2O)}$ is greater than $k_{eff(SCIs+HCOOH)}$, which, in turn, is greater than $k_{eff(SCIs+SO2)}$.

(f) The saturated vapour pressure and saturated concentration of the adduct products formed from the successive reactions of SCIs with HCOOH decrease significantly as the number of SCIs is increased. The adduct products in the nCH$_2$OO + HCOOH reactions belong to IVOC when the number of SCIs is greater than or equal to 3. The adduct products in the nanti-CH$_3$CHOO + HCOOH, nsyn-CH$_3$CHOO + HCOOH, and n(CH$_3$)$_2$COO + HCOOH reactions belong to IVOC when the number of SCIs ranges from 2 to 4, whereas they belong to SVOC when the number of SCIs is equal to 5.

References

Caravan, R. L., Vansco, M. F., Au, K., Khan, M. A. H., Li, Y. L., Winiberg, F. A. F., Zuraski, K., Lin, Y. H., Chao, W., Trongsiriwat, N., Walsh, P. J., Osborn, D. L., Percival, C. J., Lin, J. J. M., Shallcross, D. E., Sheps, L., Klippenstein, S. J., Taatjes, C. A., and Lester, M. I.: Direct kinetic measurements and theoretical predictions of an isoprene-derived Criegee intermediate, Proc. Natl. Acad. Sci. U.S.A., 117, 9733-9740, https://doi.org/10.1073/pnas.1916711117, 2020.

Chao, W., Hsieh, J. T., Chang, C. H., and Lin, J. J. M.: Direct kinetic measurement of the reaction of the simplest Criegee intermediate with water vapor, Science, 347, 751-754, https://doi.org/10.1126/science.1261549, 2015.

Chen, L., Wang, W., Wang, W., Liu, Y., Liu, F., Liu, N., and Wang, B: Water‑catalyzed decomposition of the simplest Criegee intermediate CH_2OO, Theor. Chem. Acc., 135, 131-143, https://doi.org/10.1007/s00214-016-1894-9, 2016.

Chung, C. A., Su, J. W., and Lee, Y. P.: Detailed mechanism and kinetics of the reaction of Criegee intermediate CH_2OO with HCOOH investigated via infrared identification of conformers of hydroperoxymethyl formate and formic acid anhydride, Phys. Chem. Chem. Phys., 21, 21445-21455, https://doi.org/10.1039/c9cp04168k, 2019.

Compernolle, S., Ceulemans, K., and Müller, J. F.: EVAPORATION: a new vapour pressure estimation method for organic molecules including non-additivity and intramolecular interactions, Atmos. Chem. Phys., 11, 9431-9450, https://doi.org/10.5194/acp-11-9431-2011, 2011.

Donahue, N. M., Kroll, J. H., Pandis, S. N., and Robinson, A. L.: A two-dimensional volatility basis set – Part 2: Diagnostics of organic-aerosol evolution, Atmos. Chem. Phys., 12, 615-634, https://doi.org/10.5194/acp-12-615-2012, 2012.

Huang, H. L., Chao, W., and Lin, J. J. M.: Kinetics of a Criegee intermediate that would survive high humidity and may oxidize atmospheric SO_2, Proc. Natl. Acad. Sci. U.S.A., 112, 10857-10862, https://doi.org/ 10.1073/pnas.1513149112, 2015.

Karton, A., Kettner, M., and Wild, D. A.: Sneaking up on the Criegee intermediate from below: Predicted photoelectron spectrum of the CH_2OO^- anion and W3-F12 electron affinity of CH_2OO, Chem. Phys. Lett., 585, 15-20, http://doi.org/10.1016/j.cplett.2013.08.075, 2013.

Khan, M. A. H., Percival, C. J., Caravan, R. L., Taatjes, C. A., and Shallcross, D. E.: Criegee intermediates and their impacts on the troposphere, Environ. Sci.: Processes Impacts, 20, 437-453, https://doi.org/10.1039/C7EM00585G, 2018.

Long, B., Bao, J. L., and Truhlar, D. G.: Atmospheric chemistry of Criegee intermediates: unimolecular reactions and reactions with water, J. Am. Chem. Soc., 138, 14409-14422, https://doi.org/10.1021/jacs.6b08655, 2016.

Nannoolal, Y., Rarey, J., and Ramjugernatha, D.: Estimation of pure component properties Part 3. Estimation of the vapor pressure of non-electrolyte organic compounds via group contributions and group interactions, Fluid Phase Equilibria, 269, 117-133, https://doi.org/10.1016/j.fluid.2008.04.020, 2008.

Nannoolal, Y., Rarey, J., Ramjugernatha, D., and Cordesb, W.: Estimation of pure component properties Part 1. Estimation of the normal boiling point of non-electrolyte organic compounds via group contributions and group interactions, Fluid Phase Equilibria, 226, 45-63, https://doi.org/10.1016/j.fluid.2004.09.001, 2004.

Novelli, A., Hens, K., Ernest, C. T., Martinez, M., Nölscher, A. C., Sinha, V., Paasonen, P., Petäjä, T., Sipilä, M., Elste, T., Plass-Dülmer, C., Phillips, G. J., Kubistin, D., Williams, J., Vereecken, L., Lelieveld, J., and Harder, H.: Estimating the atmospheric concentration of Criegee intermediates and their possible interference in a FAGE-LIF instrument, Atmos. Chem. Phys., 17, 7807-7826, https://doi.org/10.5194/acp-17-7807-2017, 2017.

Peltola, J., Seal, P., Inkilä, A., and Eskola, A.: Time-resolved, broadband UV-absorption spectrometry measurements of Criegee intermediate kinetics using a new photolytic precursor: unimolecular decomposition of CH_2OO and its reaction with formic acid, Phys. Chem. Chem. Phys., 22, 11797-11808, https://doi.org/10.1039/d0cp00302f, 2020.

Sipilä, M., Jokinen, T., Berndt, T., Richters, S., Makkonen, R., Donahue, N. M., Mauldin Iii, R. L., Kurtén, T., Paasonen, P., Sarnela, N., Ehn, M., Junninen, H., Rissanen, M. P., Thornton, J., Stratmann, F., Herrmann, H., Worsnop, D. R., Kulmala, M., Kerminen, V. M., and Petäjä, T.: Reactivity of stabilized Criegee intermediates (sCIs) from isoprene and monoterpene ozonolysis toward SO_2 and organic acids, Atmos. Chem. Phys., 14, 12143-12153, https://doi.org/10.5194/acp-14-12143-2014, 2014.

Taatjes, C. A., Welz, O., Eskola, A. J., Savee, J. D., Scheer, A. M., Shallcross, D. E., Rotavera, B., Lee, E. P. F., Dyke, J. M., Mok, D. K. W., Osborn, D. L., and Percival, C. J.: Direct measurements of conformer-dependent reactivity of the Criegee intermediate CH_3CHOO, Science, 340, 177-180, https://doi.org/10.1126/science.1234689, 2013.

Vereecken, L., Harder, H., and Novelli, A.: The reaction of Criegee intermediates with NO, RO_2, and SO_2, and their fate in the atmosphere, Phys. Chem. Chem. Phys., 14, 14682-14695, https://doi.org/10.1039/c2cp42300f, 2012.

Welz, O., Eskola, A. J., Sheps, L., Rotavera, B., Savee, J. D., Scheer, A. M., Osborn, D. L., Lowe, D., Booth, A. M., Xiao, P., Khan, M. A. H., Percival, C. J., Shallcross, D. E., and Taatjes, C. A.: Rate coefficients of C(1) and C(2) Criegee intermediate reactions with formic and acetic Acid near the collision limit: direct kinetics measurements and atmospheric implications, Angew. Chem. Int. Ed., 53, 4547-4550, https://doi.org/10.1002/anie.201400964, 2014.

Welz, O., Savee, J. D., Osborn, D. L., Vasu, S. S., Percival, C. J., Shallcross, D. E., and Taatjes, C. A.: Direct kinetic measurements of Criegee intermediate (CH_2OO) formed by reaction of CH_2I with O_2, Science, 335, 204-207, https://doi.org/10.1126/science.1213229, 2012.